Available online at www.sciencedirect.com

SCIENCE DIRECT®

Sensors and Actuators A 120 (2005) 343–348

SENSORS AND ACTUATORS A PHYSICAL

www.elsevier.com/locate/sna

Compensation of the thermal influence on a high accuracy optical fibre displacement sensor

Y. Alayli, S. Topcu*, L. Chassagne, J. Viennet

Laboratoire LIRIS, CNRS-FRE2508, Université de Versailles Saint Quentin, 45 avenue des Etats-Unis, F 78035 Versailles, France

Received 7 June 2004; received in revised form 13 December 2004; accepted 14 December 2004
Available online 5 February 2005

Abstract

Thermal drifts are the main sources of error on measurements made with a high accuracy extrinsic optical fibre displacement sensor. We propose a theoretical model which can be used to calculate the influence of temperature permitting hence to correct the measurement. Our model is based on the analysis of the effect of the temperature on electronic and optoelectronic components of the sensor. The model has been experimentally validated at a mesoscopic range of accuracy ($1\sigma \sim 300$ nm) using a custom-made optical fibre sensor.

Keywords: Optical fibre sensor; Metrology; Optoelectronic; Modelling

1. Introduction

In many industrial applications, measurements and control of high accuracy displacement stages are made using extrinsic optical fibre sensors (EOFS) [1,2]. The advantages of these sensors compared to Michelson interferometers are their low cost, their size (100 μm of diameter for few millimeters length) and their simplicity. However, as optical interferometers, these sensors are sensitive to thermal drifts of the surrounding medium. In Michelson interferometry, displacement measurements consist of a wavelength counting. Thermal drifts affect refractive index of air and thereafter the wavelength of the light source. This problem is solved by measuring all the environmental parameters (atmospheric pressure, temperature, water vapor rate, carbon dioxide rate) with specific sensors and calculating the refractive index value using semi-empirical equations [3,4]. But for the EOFS no convincing solution has ever been proposed. Cook and Hamm [5] expect an uncertainty of few tens of nanometers for a thermal drift of 10^{-3} °C. The use of an optical reference signal is certainly necessary but does not solve the problem of the thermal drifts because the measurement and the reference signals do not have necessary the same electronic circuit. Shimamoto and Tanaka [6] put forward a differential measurement method between two identical sensors measuring the same optical power reflected by a mirror. Although they observed a drift of 400 nm/°C for each sensor, they show that the drift of the unit is only 4 nm/°C. These sensors allow an instantaneous nanometric accuracy displacement measurements. However, their long term accuracy and reproducibility remained unquantified.

In a previous work, we have developed an EOFS [7]. We show that with a good metrological calibration, it is possible to use it to measure displacements with a nanometric accuracy in a controlled environment. In spite of the particular care taken in the electronic circuits and the photodetection system, the long-term stability (1500 s) of this sensor is about 12 nm. In this paper, we present an optoelectronic model describing the behavior of the EOFS according to the variations of the room temperature during the measurement. Taking into account the capability of this type of sensor, only the first order terms for each parameter have been considered. Experimental results obtained for a range of temperature from 5 to 45 °C are in good agreement with the suggested model at a mesoscopic range ($1\sigma \sim 300$ nm).

* Corresponding author. Tel.: +33 139253023; fax: +33 139253025.
E-mail address: suat.topcu@ens-phys.uvsq.fr (S. Topcu).

0924-4247/$ – see front matter
doi:10.1016/j.sna.2004.12.019

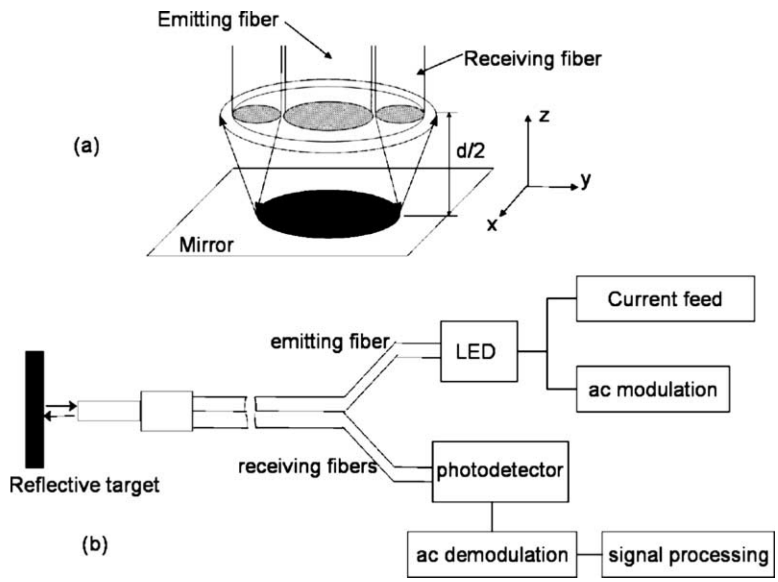

Fig. 1. Principle of the amplitude-modulated optical fibre displacement sensor. (a) The geometrical configuration of a fibre optic based sensor and (b) the different elements of the sensor.

2. Analysis of sensitivity of the optoelectronic components

The principle of intensity modulated optical fibre displacement sensors is well documented [8–11]. The light from an infrared LED is conveyed by the emitting fibre onto the target forming a circular pool of light (Fig. 1(a)). A portion of the reflected light couples into the receiving fibres and its intensity is measured by a silicon photodiode at the other end of the fibre. If the target distance z is zero, all the light is reflected back into the emitting fibre and the received signal would be null. As z increases, more and more light is coupled into the receiving fibres, up to a distance where the detected intensity reaches a peak. Fig. 1(b) shows sketch of a conventional EOFS which is ac modulated. It is composed of an ac modulated optical source, multimode optical fibres that transmit the light, a mechanical assembly integrating optical probes, a photodiode detecting the optical power and an analog signal processing electronic circuit. The sensitivity of the sensor is defined by

$$S(\xi) = \frac{\mathrm{d}P_{\mathrm{r}}(\xi)}{\mathrm{d}\xi} \tag{1}$$

where P_{r} is the power received by the photodiode for a distance ξ between emitting and receiving fibres. The stability of these sensors is limited by the thermal drifts of the transmitter, of the photodiode, of the mechanical assembly integrating optical probes, and of the processing electronic circuits. Stability is also dependent on the bending of optical fibres that induces optical power losses. The standard uncertainty on displacement values is a function of these drifts. The estimation of errors on measurements due to thermal drifts allows the limits of these sensors to be calculated.

2.1. Effect of temperature on the transmitter

The light source is generally a non-cooled infrared light emitting diode unregulated in temperature. Its common characteristics are a center wavelength (λ) included between 780 and 850 nm, a spectral width (Γ) of tens of nanometers, and an optical output power (P_{e}) of tens of microwatts. The beam is collimated with a short focal lens to have a narrow diameter of radiation. A non-coherent light source is used to avoid interference effects between a front face of the optical probe and the reflective surface, forming a Fabry Perot cavity. An increase of the surrounding temperature decreases the optical power P_{e}, broadens the emission spectrum, and translates the wavelength of the central peak. Hence optical output power of the light source could be represented as a function $P_{\mathrm{e}} = P_{\mathrm{e}}(T, \lambda, \Gamma)$. Relative variation of P_{e} is given by

$$\frac{\Delta P_{\mathrm{e}}}{P_{\mathrm{e}}} = \alpha_{\mathrm{T}}\Delta T + \alpha_{\lambda}\Delta\lambda + \alpha_{\Gamma}\Delta\Gamma \tag{2}$$

where

$$\alpha_{\mathrm{T}} = \frac{1}{P_{\mathrm{e}}}\left(\frac{\partial P_{\mathrm{e}}}{\partial T}\right)_{\lambda,\Gamma} \tag{3}$$

$$\alpha_{\lambda} = \frac{1}{P_{\mathrm{e}}}\left(\frac{\partial P_{\mathrm{e}}}{\partial \lambda}\right)_{T,\Gamma} \tag{4}$$

$$\alpha_{\Gamma} = \frac{1}{P_{\mathrm{e}}}\left(\frac{\partial P_{\mathrm{e}}}{\partial \Gamma}\right)_{T,\lambda} \tag{5}$$

Table 1
Commercial characteristics of the optoelectronic and electronic components

Designation	Characteristic	Nominal value
Preamplifier and amplifier AD645[a]	$V_0^\ddagger$	250 μV
	$\alpha_{V_0^\ddagger}$	1 μV/°C
	I_b	1.5 pA
	α_{I_t}	50 pA/°C
	ΔG	50 ppm/°C
	$V^\ddagger$	280 μV
	$\alpha_{V^\ddagger}$	10 μV/°C
Photodiodes HFD3022[b]	S_p	0.52 A/W
	α_{S_p}	-2×10^{-4} (A/W)/°C
	α_{λ_p}	1×10^{-4} nm^{-1}
	I_d	50 pA
LED HFE4050[c]	α_T	-8×10^{-3} °C^{-1}
	α_λ	-5×10^{-4} nm^{-1}
	α_Γ	15×10^{-4} nm^{-1}
	$\Delta\lambda$	3 nm/°C
	$\Delta\Gamma$	0.7 nm/°C
Mechanic	α_m	10^{-5} °C^{-1}
Thin film	α_{R_f}	−100 ppm/°C

[a] Datasheet Analog Devices AD645 RevB, 1991.
[b] Datasheet Honeywell HFD3022, 1998.
[c] Datasheet HFE4050, 1998.

and

$$\Delta\lambda = \left(\frac{d\lambda}{dT}\right)\Delta T \tag{6}$$

$$\Delta\Gamma = \left(\frac{d\Gamma}{dT}\right)\Delta T \tag{7}$$

The typical values of α_T, α_λ and α_Γ are reported in Table 1. Taking into account all theses parameters in Eq. (2), one can show that an increase of 1 °C of the room temperature will induce an optical power variation of approximately −1%.

2.2. Effect of temperature on the sensitivity of the photodiode

The sensitivity of photodiodes depends on the room temperature and the wavelength (λ_p) of the central peak of the detected light. The absorption spectrum of the silicium photodiodes is strongly non-gaussian and presents a maximum around 850 nm at 25 °C. If the sensitivity is defined by $S_p = S_p(T, \lambda_p)$, the relative variation $\Delta S_p/S_p$ is then given by

$$\frac{\Delta S_p}{S_p} = \alpha_{S_p}\Delta T + \alpha_{\lambda_p}\Delta\lambda_p \tag{8}$$

where

$$\alpha_{S_p} = \frac{1}{S_p}\left(\frac{\partial S_p}{\partial T}\right)_{\lambda_p} \tag{9}$$

$$\alpha_{\lambda_p} = \frac{1}{S_p}\left(\frac{\partial S_p}{\partial \lambda_p}\right)_T \tag{10}$$

and

$$\Delta\lambda_p = \left(\frac{d\lambda_p}{dT}\right)\Delta T \tag{11}$$

The typical values for a silicium photodiodes are reported in Table 1. For example, if room temperature increases by an amount of 1 °C, the sensitivity S_p will change by a quantity of −0.07%.

2.3. Effect of temperature on the mechanical assembly

The optical probe is integrated in a metal case and positioned orthogonally to a reflective surface. The mechanical assembly supporting the reflective surface consists generally of iron or steel whose linear expansion coefficient is about 10^{-5} °C^{-1}. For a distance of 100 μm between the probe and the mirror, a systematic error of 1 nm is induced when the room temperature fluctuates by 1 °C. Furthermore, optical fibres are prone to stretching and bending that can induce losses of optical power conveyed in the fibres. In the case of EOFS with ac modulation, variations of temperature affect mainly the propagation modes of the light when the optical fibres are curved [12].

2.4. Analog signal processing

The photodiode is associated with a load resistance R_f, a low noise preamplifier and a low noise amplifier. The output voltage of the sensor $V^\dagger$ is given by

$$V^\dagger = GV_0 + V^\ddagger \tag{12}$$

where G is the gain, $V^\ddagger$ is the offset voltage of the amplifier. The voltage at the output of the preamplifier V_0 is given by

$$V_0 = R_f(T)S_p(T, \lambda_p)P_r(\xi, T) + R_f(T)I_t(T) + V_0^\ddagger \tag{13}$$

where $V_0^\ddagger$ is the offset voltage of the preamplifier, P_r is the optical power reflected by the target mirror and conveyed by the receiving optical fibres, and

$$I_t = I_b + I_d \tag{14}$$

is the total current composed of I_b the polarization current and I_d the dark current of the photodiode. When the room temperature varies from T to $T + \Delta T$, the variation of V_0 can be expressed by

$$\Delta V_0 = \frac{\partial V_0(\xi, T)}{\partial\xi}\Delta\xi + \frac{\partial V_0(\xi, T)}{\partial T}\Delta T \tag{15}$$

where

$$\Delta\xi = \left(\frac{d\xi}{dT}\right)\Delta T$$

$$\frac{\partial V_0(\xi, T)}{\partial\xi}\Delta\xi = \frac{\partial P_r(\xi)}{\partial\xi}R_f S_p \Delta\xi \tag{16}$$

and

$$\frac{\partial V_0(\xi,T)}{\partial T}\Delta T=\left[\frac{\partial P_\mathrm{r}}{\partial T}S_\mathrm{p}R_\mathrm{f}+\frac{\partial R_\mathrm{f}}{\partial T}(S_\mathrm{p}P_\mathrm{r}+I_\mathrm{t})+\frac{\partial S_\mathrm{p}}{\partial T}P_\mathrm{r}R_\mathrm{f}+\frac{\partial I_\mathrm{t}}{\partial T}R_\mathrm{f}+\frac{\partial V_0^{\ddagger}}{\partial T}\right]\Delta T. \quad (17)$$

So, ΔV_0 can be rewritten as

$$\Delta V_0=\frac{\partial P_\mathrm{r}(\xi)}{\partial \xi}R_\mathrm{f}S_\mathrm{p}\Delta\xi+[(\alpha_{R_\mathrm{f}}+\alpha_{S_\mathrm{p}}+\alpha_\mathrm{T})P_\mathrm{r}S_\mathrm{p}R_\mathrm{f}+(\alpha_{R_\mathrm{f}}+\alpha_{I_\mathrm{t}})I_\mathrm{t}R_\mathrm{f}+\alpha_{V_0^{\ddagger}}V_0^{\ddagger}]\Delta T \quad (18)$$

where

$$\alpha_{R_\mathrm{f}}=\frac{1}{R_\mathrm{f}}\left(\frac{\partial R_\mathrm{f}}{\partial T}\right) \quad (19)$$

$$\alpha_{I_\mathrm{t}}=\frac{1}{I_\mathrm{t}}\left(\frac{\partial I_\mathrm{t}}{\partial T}\right) \quad (20)$$

$$\alpha_{V_0^{\ddagger}}=\frac{1}{V_0^{\ddagger}}\left(\frac{\partial V_0^{\ddagger}}{\partial T}\right) \quad (21)$$

represent, respectively, the thermal drift coefficients due to load resistance R_f, to the input polarization, to the total current, and to the offset voltage.

Finally, $\Delta V^{\dagger}$ takes the form

$$\Delta V^{\dagger}=G\Delta V_0+V_0\Delta G+\alpha_{V^{\ddagger}}V^{\ddagger}\Delta T \quad (22)$$

where

$$\alpha_{V^{\ddagger}}=\frac{1}{V^{\ddagger}}\left(\frac{\partial V^{\ddagger}}{\partial T}\right)$$

$$\Delta G=\left(\frac{\mathrm{d}G}{\mathrm{d}T}\right)\Delta T. \quad (23)$$

The variations of the output voltage of the EOFS according to the temperature could be calculated using Eqs. (18) and (23).

3. Experimental results

To validate our model, we use the EOFS developed in our laboratory. The incoherent light source used in our system is a gallium aluminium arsenide infrared light emitting diode from Honeywell (e.g. HFE4050, $\lambda_0 \approx 850$ nm). The optical power is 40 μW. A high stability voltage reference is used to drive the LED and so to prevent a power drift. Furthermore, the power of the light source is modulated at a frequency of 30 kHz by a high stability oscillator that improves the signal to noise ratio over a wide bandwidth. In our configuration, there are four receiving fibres placed in a star configuration around the emitting fibre, increasing hence the sensitivity of the sensor. The emitting and receiving fibres are multimode and step index fibres with a numerical aperture of 0.43. The core diameter of the emitting and receiving fibres are, respectively, 200 and 100 μm. We use a HFD3022 (Honeywell) photodiode because of its low dark current. A low input noise operational amplifier in a current to voltage configuration allows to achieve the nanometric resolution. The photodetection electronic circuit is adjusted to have a sensitivity equal to 30 μV/nm. This sensor has been calibrated by the National Institute of Metrology (BNM-LNE, France). The calibration shows a short term accuracy of ±3.5 nm (at 1σ) and a long term accuracy of ±12.2 nm.

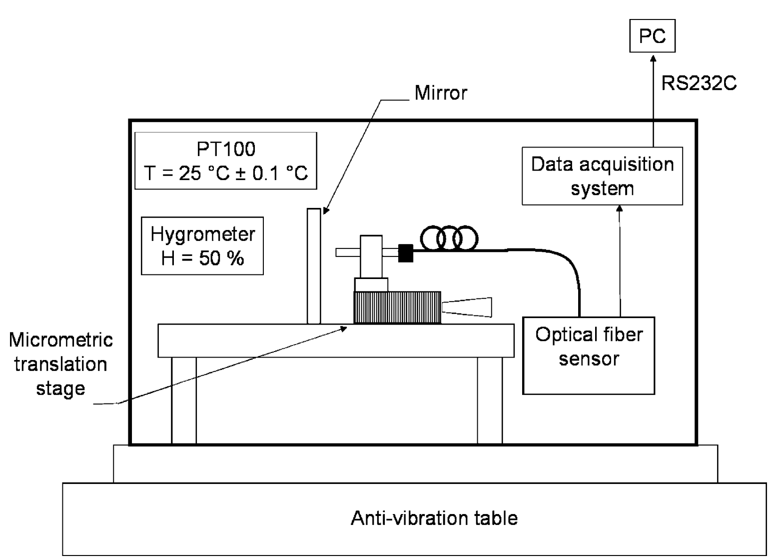

Fig. 2. Experimental setup for the study of the effect of the temperature on the optical fibre sensor.

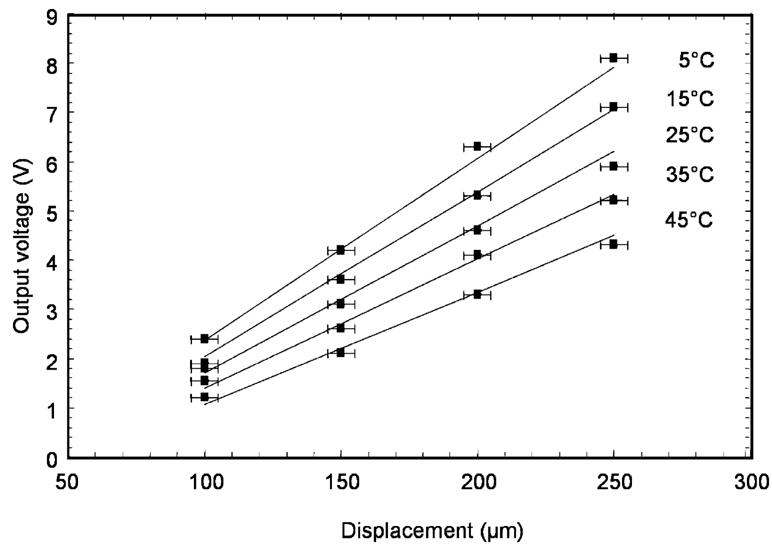

Fig. 3. Output voltage of the sensor as a function of the displacement for different temperatures: 5, 15, 25, 35 and 45 °C. (—) Values calculated by the model and (■) experimental value and its standard deviation.

3.1. Effect of the temperature on the sensitivity of the sensor

To study the influence of temperature on the sensitivity of the sensor, the EOFS is installed in a drying oven whose temperature is adjustable from 0 to 100 °C (Fig. 2). A temperature sensor (platinum resistance) measures the temperature at a thermodynamic equilibrium with an uncertainty of 0.1 °C. The relative humidity content and the atmospheric pressure are controlled to be respectively, 50 ± 1% and 1,013,300 Pa. The optical probe is mounted on a micrometric translation stage and a mirror is fixed perpendicularly to the head of the sensor. All the system is put on an anti-vibration table to be free from mechanical disturbances. Gloves give access to the thumb screw to make mechanical displacement. The uncertainty on the position is about 5 μm. A null displacement is obtained when the head of the optical probe is completely put against the mirror. The output voltage $V^{\dagger}$ of the EOFS is measured over the linear displacement range [100 μm, 250 μm] with a step equal to 50 μm. The selected temperatures are 5, 15, 25, 35 and 45 °C. The measurements are recorded using a high-accuracy voltmeter (HP 34401A, Helwett Packard) with a resolution of 100 nV. Results are depicted in Fig. 3. Each point represents an arithmetic mean value over 100 s (i.e. ∼1000 points). Absolute standard deviation (1σ) is about 0.01 V. Straight lines represent the variation of the sensitivity calculated using our model. Manufacturing values of the characteristics of the electronic and optoelectronic compo-

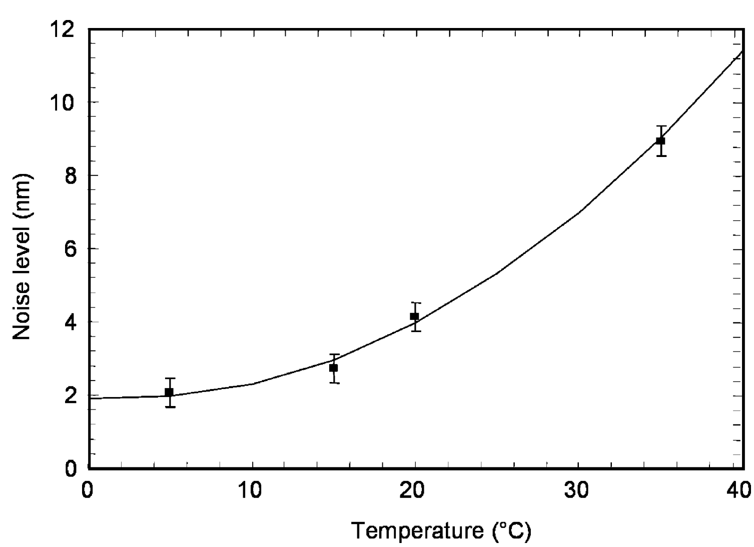

Fig. 4. Electronic noise level of the sensor as a function of the room temperature.

nents used are given in Table 1. The experimental results and the optoelectronic model are in a good agreement. As predicted by the model, the sensitivity of the sensor decreases when the temperature increases. The main components which determine the behavior of the sensor are the LED and the photodiode.

3.2. Effect of the temperature on the electronic noise level

The minimum target displacement measurable (or resolution) is an important characteristic of the sensor. The resolution of the EOFS is calculated from the noise level of the electronic circuit. It is determined for each temperature using $V^{\dagger}/V_n = 1$ where V_n is the noise level voltage. For this purpose, the LED is switched off and the noise level is measured through a low-pass fourth order filter with a time constant of 100 ms. The microvoltmeter is a Helwett Packard device with a resolution of 3 μV. Fig. 4 shows the resolution of the sensor as a function of temperature (5, 15, 20 and 35 °C). Each point is a mean value of 100 points with a standard deviation at 1σ. The resolution decreases while the temperature increases. At a standard temperature of 25 °C, the resolution of the sensor is 5 nm.

4. Conclusion

Measurement and control of displacements at nanometric scale requires to control the thermal drift of the surrounding medium. This drift changes the optical power of the transmitter and shifts the operated wavelength of the sensor. It is sometimes possible to control the temperature with a Peltier element. When it is not possible, the optoelectronic model we propose is very useful to take into account the effect of the temperature on the optoelectronic components of the sensor. The suggested model has been compared to experimental data obtained with an EOFS constructed in our laboratory. Experimental results obtained for a range of temperature from 5 to 45 °C are in good agreement with the suggested model at a mesoscopic range.

Acknowledgements

This research task was financed by ANVAR-Picardy and the experimental part was completed at the Roberval Laboratory of the University of Technology of Compiegne.

References

[1] H. Mizumoto, M. Yabuka, T. Shimizu, Y. Kami, An angström-positionning system using a twist-roller friction drives, Prec. Eng. 17 (1995) 57–62.
[2] C.S. Ling, R.S. Chang, Fiber optic displacement sensors for the measurement of vibrating object, Prec. Eng. 16 (1994) 302–306.
[3] K.P. Birch, M.J. Downs, An updated edlén equation for the refractive index of air, Metrologia 30 (1993) 155–162.
[4] R. Thibout, S. Topçu, Y. Alayli, P. Juncar, A transfer standard of the mètre: an air wavelength reference, Eur. Phys. J. AP 16 (2001) 239–245.
[5] R.O. Cook, C.W. Hamm, Fibre optic lever displacement transducer, Appl. Opt. 18 (1979) 3230–3241.
[6] A. Shimamoto, K. Tanaka, Optical fiber displacement sensor using ac-modulated light source with subnanometer resolution and low thermal drift, Appl. Opt. 34 (1995) 5854–5860.
[7] Y. Alayli, S. Topcu, D. Wang, R. Dib, L. Chassagne, Applications of a high accuracy optical fiber displacement sensor to vibrometry and profilometry, Sens. Actuators A 116 (2004) 85–90.
[8] C. Kissinger, Fiber optic proximity probe, US Patent 3,327,584, 1963.
[9] C.D. Kissinger, Fibre optic displacement measuring apparatus, US Patent 3,940,608, 1967.
[10] L. Hoogenboom, Theoretical and experimental analysis of a fiber proximity probe, SPIE, Fiber Optic Laser Sens. II 478 (1984).
[11] M. Jonhson, Fiber displacement sensors for metrology and control, Opt. Eng. 24 (6) (1985).
[12] S.L. Chuang, Physics of Optoelectronic Devices, John Wiley applied optics edition, 1995.

Biographies

Yasser Alayli received his PhD in applied physics from Pierre et Marie Curie University of Paris (Paris, France) in 1978. He is professor at Versailles Saint-Quentin University, France, and director of LIRIS. His research interests include precision engineering domain with sub-nanometric accuracy and nanotechnologies.

Suat Topcu was born at Louviers (France) in 1975. He received his PhD from Compiègne University of Technology (Compiègne, France) in 2001. Since 2002, he works as an assistant professor at the university of Versailles. His fields of research are interferometry, dimensional metrology, ellipsometry and recently laser cooling and trapping process.

Luc Chassagne was born in Paris, France, in 1971. In 1994, he received the Diplôme d'Ingénieur degree in "Instrumentations et Systèmes de Mesures" from the Ecole Supérieure d'Electricité, Paris, France, and the Doctorat en Sciences Physiques from the University of Paris XI, Orsay, France, in 2000 for his work in the field of atomic frequency standard metrology at the Laboratoire de l'Horloge Atomique, CNRS, Orsay, France. Since 2000, he has been with the University of Versailles St-Quentin-en-Yvelines, France, as an assistant professor in electronics. His current works include research on nanometrology.

Jacques Viennet is professor in electronics at the University of Versailles, France. He works on time–frequency metrology and particularly on hydrogen maser atomic clocks, at the Laboratoire de l'Horloge Atomique, CNRS. He has been director of the Institut Universitaire Technologique of Vélizy until 2003.